Nat Hazards (2007) 43:167–185
DOI 10.1007/s11069-007-9121-6

ORIGINAL PAPER

Adequacy of satellite derived rainfall data for stream flow modeling

Guleid Artan · Hussein Gadain · Jodie L. Smith · Kwabena Asante · Christina J. Bandaragoda · James P. Verdin

Received: 19 October 2006 / Accepted: 3 March 2007 / Published online: 16 May 2007

Abstract Floods are the most common and widespread climate-related hazard on Earth. Flood forecasting can reduce the death toll associated with floods. Satellites offer effective and economical means for calculating areal rainfall estimates in sparsely gauged regions. However, satellite-based rainfall estimates have had limited use in flood forecasting and hydrologic stream flow modeling because the rainfall estimates were considered to be unreliable. In this study we present the calibration and validation results from a spatially distributed hydrologic model driven by daily satellite-based estimates of rainfall for

G. Artan, J. L. Smith and K. Asante – work performed under USGS contract 03CRCN0001.

G. Artan (✉) · J. L. Smith · K. Asante
Early Warning and Environmental Monitoring, SAIC Contractor to U.S. Geological Survey (USGS)
Center for Earth Resources Observation and Science, 47914 252nd Street, Sioux Falls, SD 57198-0001, USA
e-mail: gartan@usgs.gov

J. L. Smith
e-mail: smithjl@usgs.gov

K. Asante
e-mail: asante@usgs.gov

H. Gadain
Regional Centre for Mapping of Resources for Development (RCMRD), Kasarani Road, Ruaraka, Nairobi, Kenya
e-mail: hgadain@fews.net; gadain@yahoo.com

C. J. Bandaragoda
Utah Water Research Laboratory, Utah State University,
8200 Old Main Hill, Logan, UT 84322-8200, USA
e-mail: cmay@cc.usu.edu

J. P. Verdin
Early Warning and Environmental Monitoring, U.S. Geological Survey (USGS)
Center for Earth Resources Observation and Science,
47914 252nd Street, Sioux Falls, SD 57198-0001, USA
e-mail: verdin@usgs.gov

sub-basins of the Nile and Mekong Rivers. The results demonstrate the usefulness of remotely sensed precipitation data for hydrologic modeling when the hydrologic model is calibrated with such data. However, the remotely sensed rainfall estimates cannot be used confidently with hydrologic models that are calibrated with rain gauge measured rainfall, unless the model is recalibrated.

Keywords Flood forecasting · Satellite-based rainfall estimates · Remotely sensed rainfall · Hydrologic modeling · Calibration · Validation · Nile River · Mekong River

Abbreviations

AMSU-B	Advanced Microwave Sounding Unit-B
CCD	Cold cloud duration
CN	Soil Conservation Service Curve Number
CPC	Climate Prediction Center
DEM	Digital elevation model
EROS	Center for Earth Resources Observation and Science
FAO	Food and Agriculture Organizations of the United Nations
FEWS	Famine Early Warning System
GDAS	Global Data Assimilation System
GeoSFM	Geospatial Stream Flow Model
GIS	Geographical Information System
GORE	Gauge-observed rainfall estimates
GTS	Global Telecommunications System
IDW	Inverse distance weighted interpolation method
IR	Geostationary thermal infrared
ITCZ	Inter-Tropical Convergence Zone
MOSCEM-UA	Multiobjective Shuffled Complex Evolution Metropolis algorithm
MRC	Mekong River Commission
NSCE	Nash-Sutcliffe Coefficient of Efficiency
NOAA	National Oceanic and Atmospheric Administration
OCHA	United Nations Office for the Coordination of Humanitarian Affairs
PET	Potential evapotranspiration
PM	Passive microwave
RMSE	Root mean square error
SBRE	Satellite-based rainfall estimates
SSM/I	Special Sensor Microwave/Imager
USGS	U.S. Geological Survey
USAID	U.S. Agency for International Development
WMO	World Meteorological Organization

1 Introduction

Floods are the most widespread climate-related hazard in the world, and historically floods have been the most prevalent cause of death from natural disasters (Jonkman 2005). As

population grows and urban development encroaches upon traditional flood plain areas, the potential for loss of life and property will rise in the coming years (Pielke and Downton 2000). Most of the human losses due to floods occur in the tropical regions of Africa, Asia, and Central America. It has been established that flood early warning systems are the most effective means to reduce the death toll caused by floods. Operational flood forecasting has traditionally been driven by a dense network of rain gauges or ground-based rainfall-measuring radars that report in real time. Until now, the paucity of the ground-based hydrometeorological data collection networks in tropical regions, significant delays in data availability in some countries, and the lack of hydrometeorological data sharing across international borders for trans-boundary basins have made it unfeasible to use traditional flood forecasting systems across large parts of the developing world.

The availability and global coverage of satellite data offer effective and economical means for calculating areal rainfall estimates in sparsely gauged regions. The use of satellite-based rainfall estimates (SBRE) in flood forecasting and hydrologic stream flow modeling has been limited in the past because of the perceived uncertainty associated with such data. Furthermore, errors in rainfall estimates may be amplified in flood forecasting models that rely on such rainfall estimates as inputs. It has been suggested by some researchers (e.g., McCollum et al. 2000) that in tropical regions the SBRE are more reliable because precipitation is usually associated with deep convection. In the past few years there has been some research on the use of SBRE for hydrologic modeling (Guetter et al. 1996; Vicente et al. 1998; Tsintikidis et al. 1999; Grimes and Diop 2003; Hossain and Anagnostou 2004; Nijssen and Lettenmaier 2004; Hughes 2006; Wilk et al. 2006).

We consider three criteria necessary to quantify the usefulness of SBRE for flood forecasting: (1) the SBRE data should have historical depth, (2) SBRE data should be readily available to the wider public, and (3) SBRE data should have a temporal resolution that is daily or more frequent. Previous studies, except Hong et al. (2006), have not met all of these criteria simultaneously. Hong et al. (2006) quantified uncertainty in the streamflow prediction from a conceptual hydrologic model forced with satellite rainfall; they quantified how the uncertainty in precipitation estimates propagates into the hydrological model. The SBRE data that Hong et al. (2006) have used were calculated with PERSIANN-CCS algorithm (Hong et al., 2004). Where Hong et al. (2006) used SBRE data with high spatio-temporal resolution (0.040 - 0.096 of a degree and 30-min time intervals) over large areas. Guetter et al. (1996) used synthetically produced SBRE. Other studies have reached conclusions based on the results from hydrologic models forced with SBRE data with a short time series (e.g., Tsintikidis et al. 1999). A Grimes and Diop (2003) study was based on SBRE data that were not widely available, and was based solely on cold cloud duration (CCD) and information from a numerical weather prediction model that employed site-specific calibration parameters. Hossain and Anagnostou (2004) reported results on a SBRE application for an event rainfall-runoff model from a small basin (116 km^2), and used passive microwave (PM) data as well as CCD-based rainfall estimates to force their stream flow model. Nijssen and Lettenmaier (2004) studied the effects of sampling errors in SBRE has on simulated hydrologic fluxes. While their study has advanced our understanding of the effects of the SBRE error, errors that are due to the periodic nature of the satellite imagery sampling, the results of the study were on a synthetic SBRE (an error field was imposed on rain measured with rain gauge).

For this study, we have selected four basins that are flood prone or are tributaries to flood prone rivers. Floods are very common in the downstream flat alluvial plains of both the Gash and Nyando basins. During 2002, over 48,000 people were displaced by floods in the Nyando basin in western Kenya (OCHA 2002). The Gash River consistently floods the city

of Kassala, Sudan, a city with a population of more than a half million. The river flooded Kassala in 1975, 1988, 1996, 1998, and most recently in July, 2003, when half of the city was under water, affecting approximately 60-70% of the city's population (OCHA 2003). In Southeast Asia, the Nam Ou and Se Done basins contribute large flows to the Mekong River, and therefore have a significant impact on the recurrent floods that have occurred in the area along the Mekong River's main stem. It will be beneficial for the Mekong River Commission (MRC) to be able to simulate in near-real time the runoff of rivers that originate in Laos, because there are often delays in the transmittal of hydrometeorological data. As recently as the summer of 2000, the lower Mekong experienced devastating floods, with estimates of more than 800 fatalities (Plate and Insisiengmay 2002).

In this study, we have investigated the usefulness and uncertainty of remotely sensed rainfall estimates for hydrologic modeling. We show the feasibility of using a rainfall-runoff model forced with SBRE for stream flow modeling at a daily time step. We present calibration and validation results for a spatially distributed hydrologic model driven by daily SBRE for four basins in East Africa and Southeast Asia. Two basins are tributaries of the Mekong River and two are tributaries of the Nile River. The four basins cover a wide range of physiographic and climatic conditions. For the two Mekong tributaries, rain gauge data were also available. The results demonstrate the usefulness of remotely sensed precipitation data for hydrologic modeling.

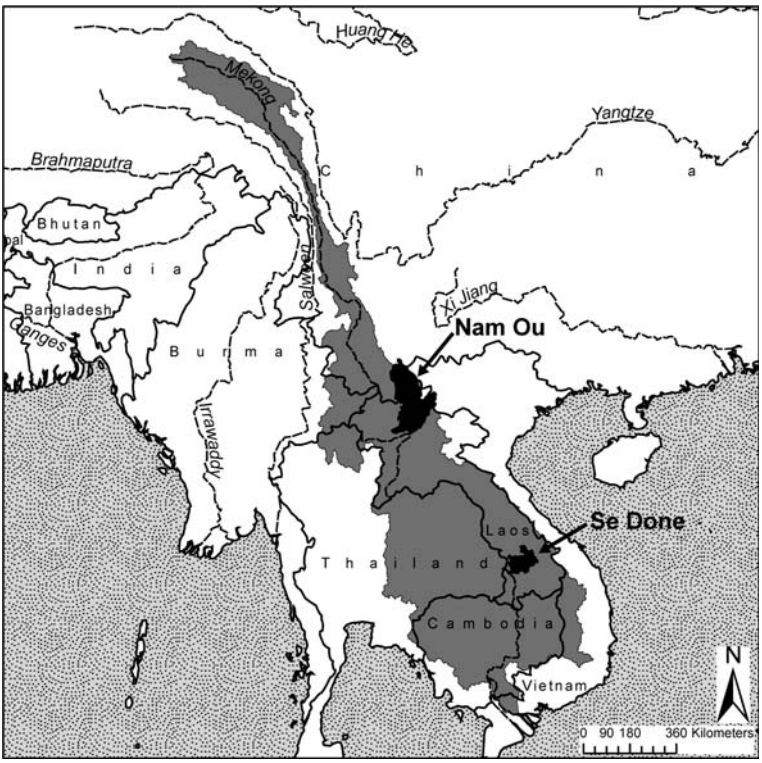

Fig. 1 Mekong River basin, with study areas shown in black: the Nam Ou basin (in the north) and the Se Done basin (in the south)

2 Study sites and models

2.1 Study sites

The Nam Ou and Se Done Rivers are tributaries of the Mekong River (Fig. 1). The Nam Ou River starts at the border between China and Laos, and flows through the rugged mountains of northern Laos, with slopes exceeding 30% in some parts of the basin. The Nam Ou basin is located in the northern highlands and has a subtropical climate, with a distinct rainy season from May through October, and a cool, dry season from November through February. Land cover is mainly forest with some agricultural land in the river valley floor. The Se Done basin is located in southern Laos in the Mekong lowland plains. The climate of the basin is tropical: hot and humid. The rainy season is mainly affected by the summer monsoon and lasts from mid-May to mid-November; most precipitation comes as short, intense thundershowers. Most of the heavy rains take place between July and September. The land cover of the basin is mainly irrigated cropland and deciduous broadleaf forest.

The Gash River is a trans-boundary basin shared among Ethiopia, Eritrea, and Sudan (Fig. 2). The river originates from the Eritrean and Ethiopian highlands in an area characterized by steep slopes; the upper course of the river in Eritrea is known as the Mareb River. The upper part of the basin has a cool climate with an average temperature of 16°C year round, whereas the lower section of the basin is dry and hot. Most of the rainfall falls in the upper part

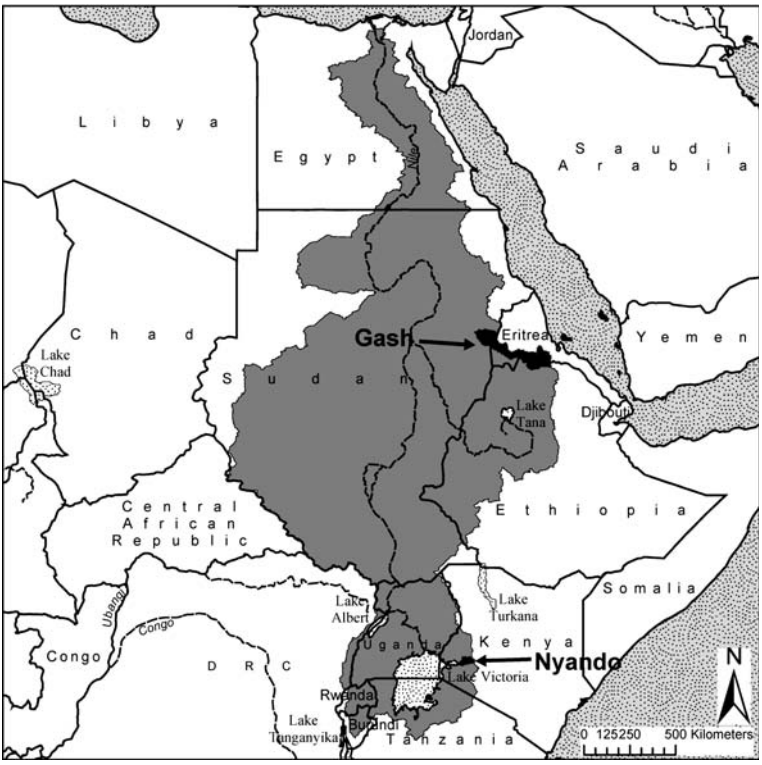

Fig. 2 Nile River basin, with study areas shown in black: the Gash River basin (in the north) and the Nyando basin (close to Lake Victoria)

of the basin. The Gash River is discontinuous in Kassala, Sudan, and during the flood season its water has high silt content, whereas the first 150–200 km of the river in Eritrea is a perennial river. The Gash River reaches the Atbara, a tributary of the Nile, only during the flood season. Almost all of the rainfall over the Gash basin falls during the rainy season from July to September. Figure 3 shows the number of days per year in which water flows in the Gash River at the Kassala gauging station. The soil in the downstream part of the basin is composed mainly of thick alluvial deposits of silty clay loam.

The Nyando River is located in western Kenya and drains into Lake Victoria (Fig. 2). The climate of the Nyando catchment is classified as sub-humid. Mean annual rainfall varies from 1200 mm close to Lake Victoria to 1500 mm at the foot of the Nyando Escarpment. The annual rainfall pattern shows no distinct dry season; it is bi-modal with peaks during the long rainy season of the region (March–May) and during the short rainy season (October–December). The rainfall in the area is controlled by the northward and southward movement of the Inter-Tropical Convergence Zone (ITCZ). The soils of the basin are mainly vertisols and entisols, medium to heavy clay soils with poor drainage; as a result, the drainage capacity in both the vertical and deep lateral directions is poor. The catchment lies between 1140 m and 1800 m above sea level, with flat topography near the lake. The vegetation of the upper catchment is mainly forest, while the middle part of basin has been greatly modified by clearing, cultivation, and burning due to human settlement. Table 1 summarizes the physiographic and climatic characteristics of the four basins in this study.

The basin boundaries and stream networks were delineated from the U.S. Geological Survey (USGS) GTOPO30 digital elevation database (http://edcdaac.usgs.gov/gtopo30/gtopo30.html). The GTOPO30 global topographic data set (Gesch et al. 1999) has a 30-arc-second resolution. In this study we subdivided the Nam Ou and Se Done into three sub-basins each. The Gash, which covers an area with several distinct climatic conditions, was divided into 62 sub-basins. The Nyando basin was modeled as 10 sub-basins.

2.2 Rainfall-runoff model

We used the Geospatial Stream Flow Model (GeoSFM) for hydrologic simulation. The GeoSFM is a physically-based semi-distributed hydrologic model developed by the USGS (Artan et al. 2001). The GeoSFM simulates the dynamics of runoff processes by using remotely sensed and widely available global data sets. The model is parsimonious; it has few parameters and variable input data requirements. The GeoSFM is a catchment-scale hydrologic model. The model consists of (a) a Graphical User Interface (GUI) component

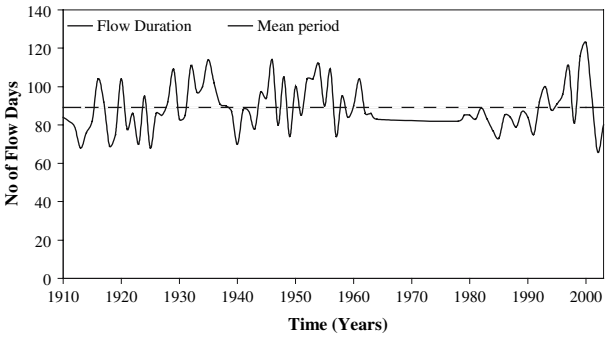

Fig. 3 Number of days in the year that the Gash River flows at Kassala, Sudan

Table 1 Basins used in this study

Basin	Area (km^2)	Climate
Se Done	6,044	Tropical
Nam Ou	19,013	Sub-tropical
Nyando	2,646	Sub-humid
Gash	22,150	Semi-arid

run within a Geographical Information System (GIS) for input data preparation and visualization of model outputs, and (b) a rainfall-runoff simulation component. In the preprocessing module, the particular basin under consideration is subdivided into several sub-basins based on the digital elevation model (DEM) data. Model parameters are derived from continental-scale datasets, and most of the parameters have physical meaning. The parameterization is accomplished through the use of three datasets describing the Earth's surface: topography, land cover, and soils.

The GeoSFM rainfall-runoff component has three main modules: water balance, catchment routing, and distributed channel routing. In the water balance module, the sub-basins are the subject of a daily water balance calculation. This calculation determines how much water enters the stream network from each sub-basin. In the water balance module, the soil is conceptualized as composed of two zones: (a) an active soil layer where most of the soil–vegetation–atmosphere interaction processes take place, and (b) the groundwater zone. The active soil layer is divided into an upper thin soil layer where evaporation and transpiration both occur and a lower soil layer where only transpiration takes place. The catchment runoff mechanisms considered in the model are excess precipitation runoff, direct runoff from impermeable areas of the basin, rapid subsurface flow (interflow), and base flow contribution from groundwater. The model has several excess runoff generation options; in the present study we used the Soil Conservation Service Curve Numbers (CN) method to model the surface runoff generation process. CN were estimated from a land use and land cover data layer, and were dynamically updated to reflect the state of the soil moisture.

The runoff produced by the water balance module is routed in two phases. First, the catchment runoff is routed at the sub-basin level to its outlet, then the flow is routed through the main river channel network. In the sub-basins, the subsurface runoff is routed using a set of two conceptual linear reservoirs. While the surface runoff routing is carried out using a diffusion wave equation modified for use in a GIS environment (Olivera and Maidment 1999), the land cover and DEM data are used to determine the rate at which runoff is transported from the point of generation to the catchment outlet. In the river channel network, water is routed using a linear Muskingum–Cunge scheme (Chow et al. 1988).

The GeoSFM has an automatic calibration toolset module that employs the Multiobjective Shuffled Complex Evolution Metropolis (MOSCEM-UA) algorithm (Duan et al. 1992; Vrugt et al. 2003). Because of uncertainties in the input and output datasets, model structure error, and quantity or quality of input, it is difficult to determine a best set of model parameters (Duan et al. 1992). The MOSCEM-UA algorithm uses a global search of the specified parameter space and has been shown to be effective and efficient. It is efficient because relatively few model runs are needed to obtain the optimal parameter set, and it is effective because it successfully deals with difficulties in the search, such as multiple local optima and derivative discontinuities. The parameter calibration method uses a complex shuffling probabilistic search procedure and a fitness assignment method for the objective function.

The number of parameters that can be adjusted in a physically based distributed hydrologic model such as GeoSFM could be excessive. In this study we limited the parameters that were adjusted during calibration to five model parameters that have shown the highest sensitivities and uncertainties in previous studies of model use. To avoid model over-parameterization, the calibration was confined to a range where model parameters were deemed to have physical meaning.

2.3 Rainfall-runoff model parameterization data and evapotranspiration

Land cover data, in conjunction with soils information, is used by the GeoSFM to parameterize how the model partitions incident rainfall between surface runoff and water that infiltrates into the soil. We used a global land cover dataset (Loveland and Belward 1997) that was created from the classification of a 12-month series of 1-km global vegetation index imagery. The soil parameters (i.e., soil water holding capacity, saturated soil hydraulic conductivity, hydrologically active soil layer depth, and soil texture) were extracted from the Digital Soil Map of the World (FAO 1995). For those attributes missing from the Food and Agriculture Organizations of the United Nations (FAO) digital soil data set, relationships described in the literature (Hanks and Ashcroft 1980; Hansen et al. 1979) were used to create them from the available attributes. The FAO digital soil data were derived from an original compilation at 1:5,000,000 scale.

Potential evapotranspiration (PET) represents atmospheric demand for water from the Earth's surface as a function of solar radiation, air temperature, wind, humidity, and atmospheric pressure. PET is an essential dataset for calculating water cycle fluxes in hydrologic modeling. We used PET data that were calculated globally on a cell-by-cell basis according to the Penman–Monteith equation (Verdin and Klaver 2002; Senay and Verdin 2003). The model is run operationally at the USGS Center for Earth Resources Observation and Science (EROS). The PET values were calculated from grids of the meteorological variables that the Penman–Monteith model requires. The meteorological data come from the Global Data Assimilation System (GDAS) dataset produced by the National Oceanic and Atmospheric Administration (NOAA) on a 1-degree by 1-degree grid.

2.4 Satellite-based rainfall estimates

In recent years, several SBRE products have been presented in the literature (Guetter et al. 1996; Herman et al. 1997; Xie and Arkin 1997; Vicente et al. 1998; Tsintikidis et al. 1999; Grimes and Diop 2003; Hong et al. 2004; Joyce et al. 2004, Huffman et al. 2007). In this research we used an operational SBRE that the National Oceanic and Atmospheric Administration (NOAA) Climate Prediction Center (CPC) has produced since January, 1996; for the Famine Early Warning System (FEWS) project of the U.S. Agency for International Development (USAID). From 1998 to 2000, the NOAA/CPC produced SBRE version 1.0, based on the algorithms of Herman et al. (1997). From January 2001, to the present, SBRE version 2.0 has been in production (Xie and Arkin 1997). A SBRE product with a spatial resolution of 10 km by 10 km and daily temporal resolution has been produced for windows that cover Africa, central Asia, and southern Asia (see Fig. 4). The public can access this SBRE data for the three geographical areas from an anonymous ftp site at ftp://ftp.cpc.ncep.noaa.gov/fews. The daily SBRE data for the African window extends as far back as January 1, 1998; for southern and central Asia, the starting date was January 10, 2001.

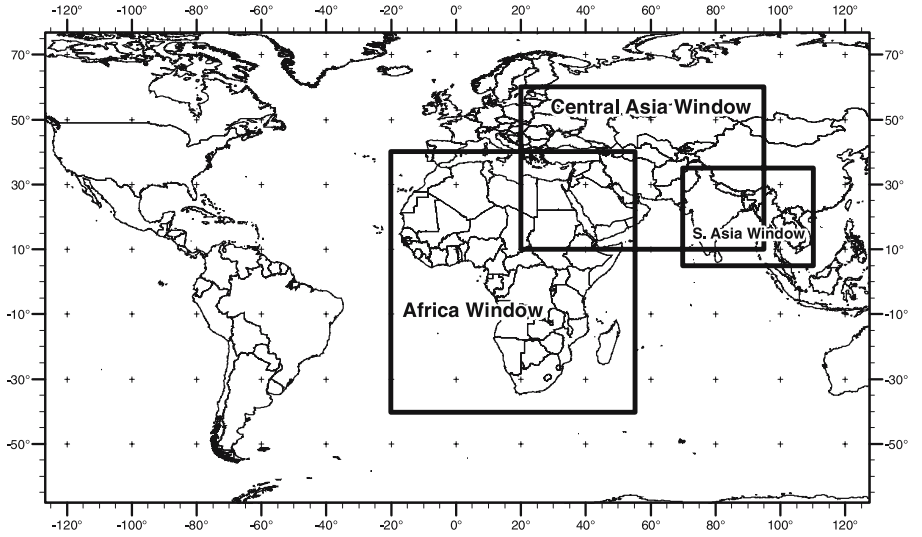

Fig. 4 Geographic extent of areas where the NOAA/CPC satellite-based rainfall estimate products are available

The basic inputs for creation of the SBRE product are geostationary thermal infrared (IR) satellite imagery, passive microwave (PM) imagery, and daily rain gauge reports from the Global Telecommunication System (GTS) of the World Meteorological Organization (WMO). For version 1.0, rainfall was estimated from cold cloud duration (CCD) calculated with a temperature threshold of 235 K from the IR imagery, ingested on a half-hourly basis and aggregated on a daily time step, with bias removed from the IR-based rainfall estimates using interpolated GTS rainfall fields (Herman et al. 1997). Usually the GTS data are sparser in the areas where benefits from the SBRE product could be the highest. For the southern Asia window there are up to 1,749 stations that are part of the GTS reporting network, but for any given day about 600 stations were used to make the SBRE product. There are 2,534 GTS stations for the African window and 4,146 stations for the central Asia window, with the usable number of stations close to 1,000 and 500 stations, respectively.

Since January 2001; the NOAA/CPC has produced the SBRE version 2.0, which incorporates additional satellite data from two instruments, the Special Sensor Microwave/ Imager (SSM/I) of the Defense Meteorological Satellite Program, and the Advanced Microwave Sounding Unit-B (AMSU-B) on board polar orbiting satellites NOAA-15, NOAA-16, and NOAA-17. The SSM/I estimates are acquired at 6-h intervals, while AMSU-B rainfall estimates are made every 12 h. In this method, rainfall is first estimated separately from the three satellite sources with a maximum likelihood approach that uses weighting coefficients that are inversely proportional to the squares of the individual data random errors. Finally, the satellite rainfall estimates are merged with interpolated rainfall from the available GTS station data so that the satellite data provide the field shape and are anchored by the GTS data. The PM data strengthen the rainfall estimate because there is a more direct physical relationship between rainfall and the signal at the satellite, compared to the IR data. The shortcoming of the PM data is the lower frequency of observation and coarser spatial resolution compared to the IR images from geostationary satellites. The NOAA/CPC SBRE products have been previously used to model crop water requirements (Verdin and Klaver 2002; Senay and Verdin 2003).

2.5 Gauge observed data

The rainfall station data and streamflow gauge data for the Nam Ou and Se Done basins were supplied by the Mekong River Commission (MRC). The MRC is a regional international river basin organization created by Cambodia, Lao PDR, Thailand, Vietnam, and Myanmar. The data covered the period from January 1990 to December, 2003. The gauge-observed rainfall estimates (GORE) were interpolated onto a 10-km grid using a simple inverse distance-weighting algorithm (IDW). Tables 2–4 summarize the location and temporal coverage of the GORE data. Missing data for a particular day were excluded from the interpolation process, reducing the number of gauges for that day. As shown by Tables 2 and 3, the smaller Se Done basin had more rain gauge coverage than the larger Nam Ou basin. The number of rain gauges in and around Nam Ou was low and they were poorly distributed over the basin. All the gauges in Nam Ou Basin, except one gauge at Phongsaly,

Table 2 Location and percent of missing data of the rain gauges used for model forcing for Nam Ou basin

Stations ID	Station name	Long.	Lat.	% missing data
190202	Luang Prabang	102.13	19.88	0%
200101	Muong Namtha	101.40	20.93	0%
200201	Muong Ngoy	102.60	20.57	0%
200204	Oudomxay	102.00	20.68	0%
210201	Phongsaly	102.20	21.73	0%

Table 3 Location and percent of missing data of the rain gauges used for model forcing for Se Done basin

Stations ID	Station name	Long.	Lat.	% missing data
150504	Pakse	105.78	15.12	0%
150506	Khongsedone	105.80	15.57	0%
150508	Selabam	105.82	15.38	0%
150604	Laongam	106.17	15.47	0%
150607	Nikhom	106.43	15.18	0%
160504	Ban Donghen	105.78	16.00	0%
160601	Muong Tchepon	106.23	16.03	0%

Table 4 Location and percent of missing data of the rain gauges used for model forcing for Nyando basin

Stations ID	Station name	Long.	Lat.	% missing data
9035148	Koru Mission	35.27	−0.20	3%
9035075	Kericho	35.38	−0.33	3%
9035020	Lumbwa	35.47	−0.20	3%
9034086	Ahero	34.93	−0.15	3%
9034007	Miwani Sugar	34.95	−0.052	25%
8935159	Ainabkoi	35.33	0.082	25%
8935161	Nandi Hills	35.15	0.08	3%
8935148	Kipkurere	35.43	0.07	3%
8935033	Savani estate	35.10	0.05	3%
8935001	Songhor	35.30	0.032	22%
9034009	Miwani	34.95	−0.051	11%

were located in the lower part of the basin or close to the lower basin. We had GORE data for the Nyando basin for the period between January 1986 and December 1988.

GeoSFM-simulated streamflow was calibrated and validated using discharge data collected at station 100102, located in the town of Muong Ngoy on the Nam Ou River (with an upstream area of around 19,000 km^2), and station 390104 at Souvanna Khili for the Se Done River (upstream area about 6,000 km^2). The Gash River stream gauge data were supplied by the Sudan Ministry of Irrigation and Water Resources, for the period from January 1998 to December 2002. The Gash stream discharge data were collected at the Kassala town gauging station. The Nyando River stream gauge data were supplied by the Kenya Ministry of Water Resources and Development, for the periods January 1986 to December 1988 and January 1998 to December 2001. The discharge data were from the gauging station at Ahero Bridge (station ID 1GD03).

3 Performance indicators

We made visual and statistical comparisons between predicted and observed flows, and between SBRE and GORE averages basin-wide whenever data were available. For the statistical ''goodness of fit'' of simulated flows, we used a widely used measure—the Nash-Sutcliffe Coefficient of Efficiency (NSCE) (Nash and Sutcliffe 1970) and the value of the Root Mean Square Error (RMSE). The NSCE is an improvement over the Coefficient of Determination for streamflow comparison, because it accounts for model errors in estimating the mean of the observed datasets. The NSCE is an indicator of the model's ability to predict about the 1:1 line. We used the coefficient of determination to assess the correspondence between SBRE and GORE data. For both streamflow and rainfall variables, we calculated the mean bias between gauge-observed and modeled variables. The bias or mean error of the simulated and observed variable was calculated as:

$$Bias = \frac{\sum_{i=1}^{n} (S_i - O_i)}{\overline{O}}$$

where S_i and O_i are the simulated and observed variables, for both rainfall and streamflow, and $\overline{O}$ is the mean value of the observed variable. The NSCE was calculated as:

$$NSCE = 1 - \frac{\sum_{i=1}^{n} (S_i - O_i)^2}{\sum_{i=1}^{n} \left(O_i - \overline{O}\right)^2}$$

4 Results and discussion

4.1 Comparison of satellite and gauge-based rainfall estimates

In this section, we present a comparison of concurrent GORE and SBRE mean-areal averages over the Se Done and Nam Ou basins. The datasets span the period from January 2002 to December 2003. The two rainfall estimate datasets were projected to a Lambert

equal-area azimuthal projection. The GORE data were interpolated by using the IDW interpolation method, a simple and efficient method that is part of widely available Geographic Information Systems (GIS) software. We compared both daily and monthly accumulated basin-wide average rainfall.

The coefficient of determination (r^2) of the GORE and SBRE fields was 0.51 and 0.35 on a daily time scale for Nam Ou and Se Done basins, respectively. The r^2 coefficient was quite low for both basins, and there were no discernable differences ($p = 0.05$) between the mean values of the two rainfall estimates. The Nam Ou basin average daily rainfall was 3.9 mm for the GORE and 3.7 mm for SBRE. For the Se Done basin, the daily mean values were 5.6 mm and 5.5 mm for GORE and SBRE, respectively. On monthly time scales, there was a strong correlation between the datasets for both basins (r^2 values were 0.96 and 0.85). The correlation between the remotely sensed and gauge measured rainfall was higher for the larger of the two basins (Nam Ou), despite the poorer rain gauge distribution in that basin. Our finding of high correlation and low bias from the comparison of the GORE and SBRE monthly data is consistent with the findings from some previous researchers on the accuracy of monthly accumulations of remotely sensed precipitation averaged over large areas (Xie and Arkin 1997; Sorooshian et al. 2000), but our findings contrast with those reported by Hughes (2006).

We think that the good agreement seen between the GORE and SBRE is due to the nature of the rainfall in the lower and middle Mekong basin. The spatial-temporal characteristics of the rainfall in the area are monsoonal and well organized with the wet season lasting from May to November, when it rains almost every day. Figure 5a, b show the time series for GORE and SBRE for the two basins. Although there was a good agreement between the SBRE and GORE and a negligible bias for the yearly and monthly

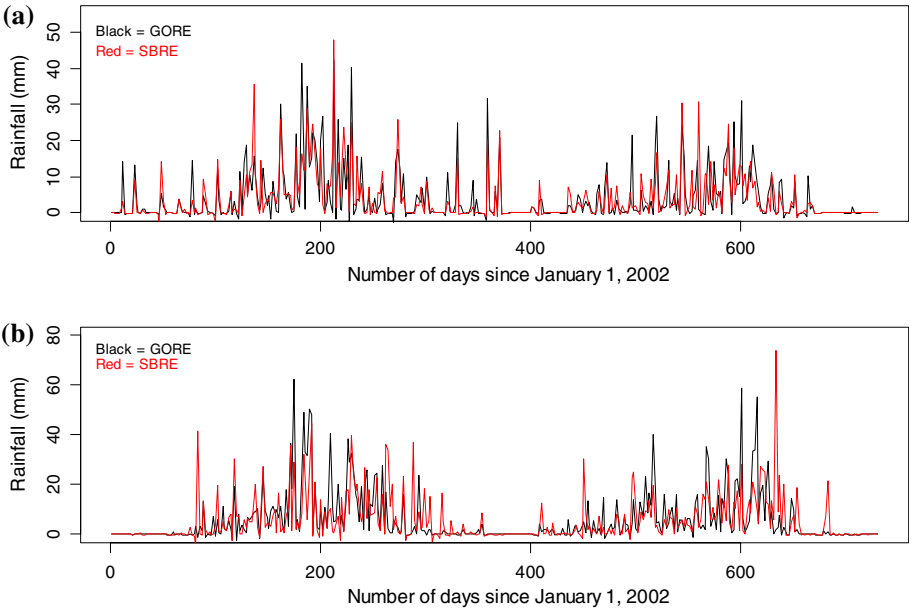

Fig. 5 Areal basin averages of remotely sensed and gauge-measured rainfall for (**a**) Nam Ou basin, and (**b**) Se Done basin

accumulated rainfall amounts, there was a small under prediction during the peak. The SBRE relies on IR and PM imagery for the rainfall estimation, and rainfall estimates made from IR and PM data have a similar bias (McCollum et al. 2000). The relationship between rainfall and the remotely sensed imagery is not well defined. Fixed temperature thresholds are used to estimate the CCD values from the IR imagery, and the PM rainfall estimates are based on empirical relationships derived by comparison with concurrent radar-estimated rainfall. The small peak rainfall biases we saw are conjectured to result from the value of the temperature threshold used to create the CCD being too low during the peak of rainy season and too high during the later part of the season. The biases in the estimates for high rainfall are apparent from Fig. 6, showing quantile–quantile (q–q) plots of the SBRE and GORE data. The plots show that the two rainfall estimate datasets have the same distribution for the lower tail, but that the SBRE has a tendency to underestimate rainfall compared to the gauges. Table 5 summarizes the results of the evaluation of the streamflow simulation when the two rainfall datasets were used.

4.2 Effects of satellite rainfall estimates on simulated streamflow

Initially, GeoSFM model parameters were estimated using digital datasets of soil, land cover, and elevation. We calibrated the GeoSFM with the GORE data for the period from 1990 to 2001 for the Nam Ou and Se Done basins, and used data from 2002 to 2003 for validation. We lacked PET data for the Mekong basin for the period before 2000. For PET during the calibration period, we used an average daily PET created by averaging the

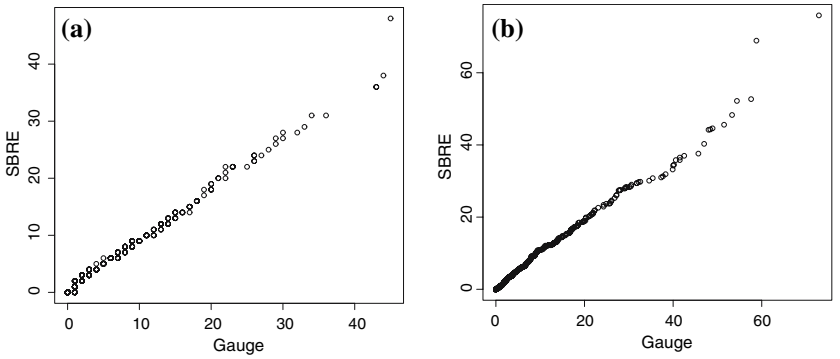

Fig. 6 Quantile–quantile (q–q) plot of the satellite-estimated and rain gauge-measured rainfall for (**a**) Nam Ou, and (**b**) Se Done basins

Table 5 Statistical summary of the comparison between simulated and observed streamflow. (a) SBRE1 model calibrated with rain gauge data and run with SBRE from a different period; (b) SBRE2 calibration output from model forced with remotely sensed rainfall estimates; and (c) GORE validation

Basin	SBRE1			SBRE2			GORE		
	NSCE	Bias (%)	RMSE	NSCE	Bias (%)	RMSE	NSCE	Bias (%)	RMSE
Se Done	0.39	37.0	13.99	0.40	0.00	12.62	0.77	11.0	7.91
Nam Ou	0.64	−29.0	14.30	0.81	−6.00	11.43	0.82	7.00	10.5
Nyando	0.46	−18.0	0.20	0.74	7.40	0.18	0.75	−8.00	0.42
Gash					0.67	−12.0	0.79		

USGS global PET datasets from 2001 to 2005. The model parameter calibration was first accomplished by trial and error and subsequently with an automatic calibration. The automatic parameter calibration routine was based on the MOSCEM-UA algorithm (Duan et al. 1992; Vrugt et al. 2003), with minimization of the RMSE as the objective function. After the calibration, the GeoSFM was forced with GORE and SBRE data for the period from January 2002 to December 2003.

The GORE calibrated model was forced with 2 years of SBRE (hereafter labeled run SBRE1). Hydrographs showing simulated and observed flows of the Se Done and Nam Ou are shown in Fig. 7a, b. The graphs show that for both basins the model was able to capture the observed hydrograph quite well when forced with GORE rainfall, simulating both the timing and the magnitude of the streamflow of the basins. The few discrepancies observed in the Nam Ou hydrograph can be explained in part by the insufficiencies of rainfall station data in the upper sections of the basin highlands. There are few noticeable differences between the hydrographs simulated with the GORE and SBRE data for the Nam Ou basin. There was poor agreement between observed and SBRE simulated streamflows for the Se Done basin.

Although the overall agreement between the SBRE and GORE accumulated rainfall was high, with only a small bias, apparently that bias was amplified in the simulated streamflow when the hydrologic model was calibrated using the GORE data. The bias of the simulated flows changed from +11% with GORE to +37% with SBRE1 for the Se Done and from +7% with GORE to −29% with SBRE1 for the Nam Ou (see Table 5). The bias of GORE-forced simulated streamflows was +12% and +11% for the two basins. Such high increases of bias and drops in prediction efficiency were present when the bias of the remotely sensed

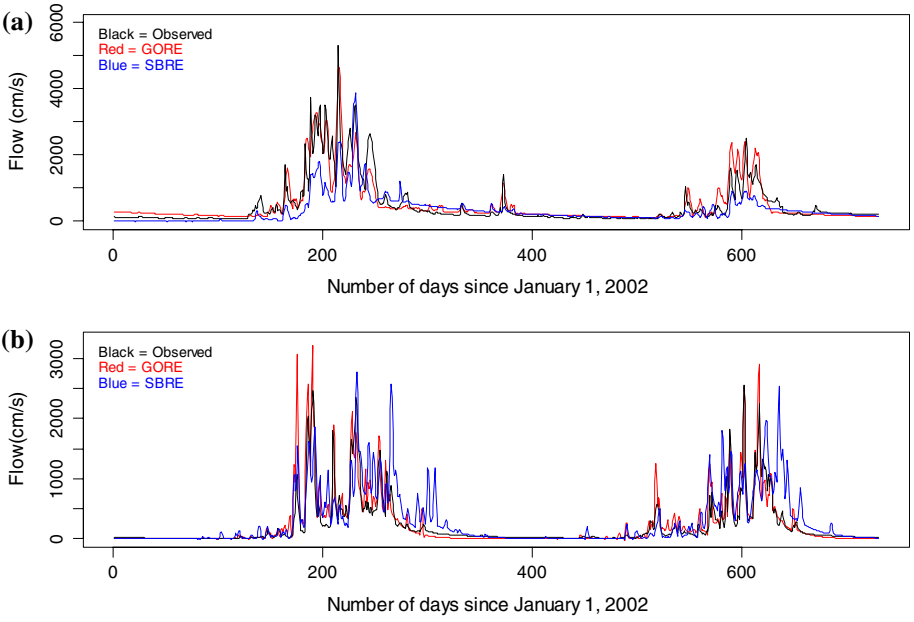

Fig. 7 Streamflow simulation obtained when the hydrologic model was calibrated with rain gauge data from the period between January 1990 and December 2001. The model was forced with mean areal rainfall from gauges and estimated from satellite imagery. The top panel (**a**) is for the Nam Ou basin and the lower panel (**b**) is for the Se Done basin

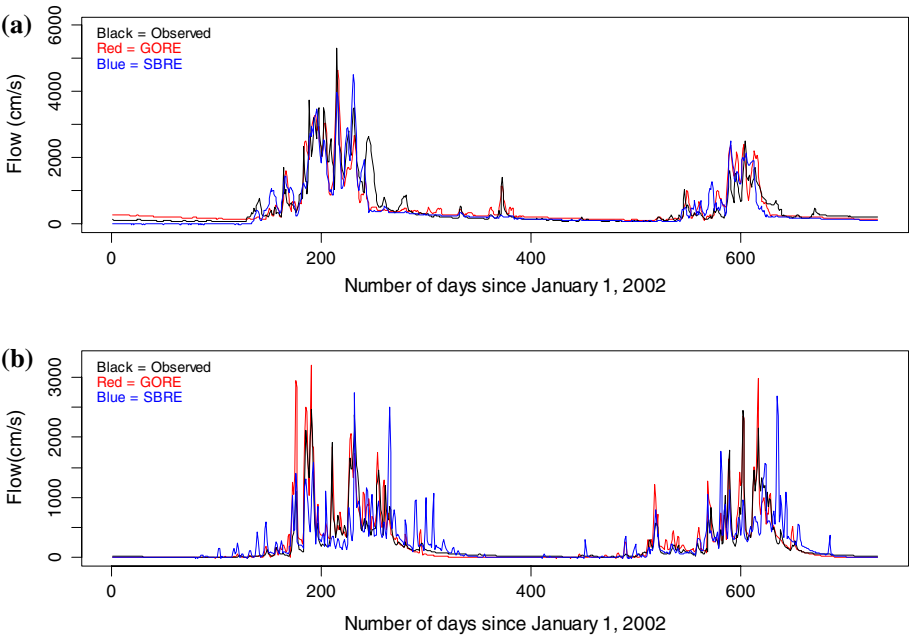

Fig. 8 Observed and simulated hydrographs obtained when the model was calibrated with SBRE data for (**a**) Nam Ou and (**b**) Se Done

rainfall was only −2% (Se Done) and −6% (Nam Ou), a mean rainfall bias that is much less than what has been reported for other areas (Guetter et al. 1996; Wilk et al. 2006).

We conclude that there was a large amplification of the rainfall bias in the simulated streamflow with SBRE1 for the Nam Ou because of the wet soil conditions expected in this area during the rainy season; any negative rainfall bias would be transformed into a larger negative bias in the simulated streamflow. In the case of Se Done basin there was a small underestimation of peak rainfall but there was a consistent overestimation of rainfall during the later part of the monsoon season (Fig. 5a). The SBRE1 run produced several peak flows in the later part of the rainy season that were not seen in the observed streamflow.

The GeoSFM was recalibrated using the SBRE as a rainfall forcing (data were from 2002 to 2003, hereafter labeled run SBRE2). Comparisons between the observed and simulated hydrographs from model run SBRE2 are summarized in Fig. 8a, b and Table 5. The bias of the simulated streamflow for Se Done decreased from +37% when the model was calibrated with GORE to 0% when the model was calibrated with SBRE, but the Nash-Sutcliffe efficiency did not increase significantly. While there was an improvement of the simulated flows in the first year, there was a deterioration of model predictive skills during the second year. The lack of improvement in efficiency indicates that the SBRE2 contains large uncertainties at the daily level that the model parameter calibration was unable to reduce significantly. The SBRE2 simulated flows for the recalibrated Nam Ou basin compared well with the observed flows. The SBRE2 runs for the Nam Ou were less biased (−6%) than the simulated flow when the model was calibrated with GORE of the same period, and the simulation efficiency was similar to the flows simulated with GORE data. The SBRE provides an adequate and comparable data source to the GORE data for flood forecasting and hydrologic modeling for the Nam Ou basin, whereas the same could not be said about the Se Done basin.

We calibrated the Nyando basin with GORE and stream gauge data collected from January 1986 to December 1988 at the Ahero Bridge gauge. We did not compare GORE and SBRE because we did not have concurrent datasets from the two sources. After the model was calibrated with the GORE, we simulated flows with the GeoSFM forced with SBRE input from January 2000 to December 2001. Then we calibrated the model with SBRE data from January 1996 to June 1997. Results of the simulated hydrograph when the model was forced with rainfall data from SBRE and GORE are illustrated in Fig. 9a, c. Simulated and observed flows agreed well most of the time (especially for the peak flows) when the model was run with GORE. There was less agreement between simulated and observed flows with SBRE1 (Fig. 9b). The hydrograph was simulated for two very different years, a wet year and a below-average flow year. The shape of the simulated hydrograph was close to the observed hydrographs during the wet year (2000) but model

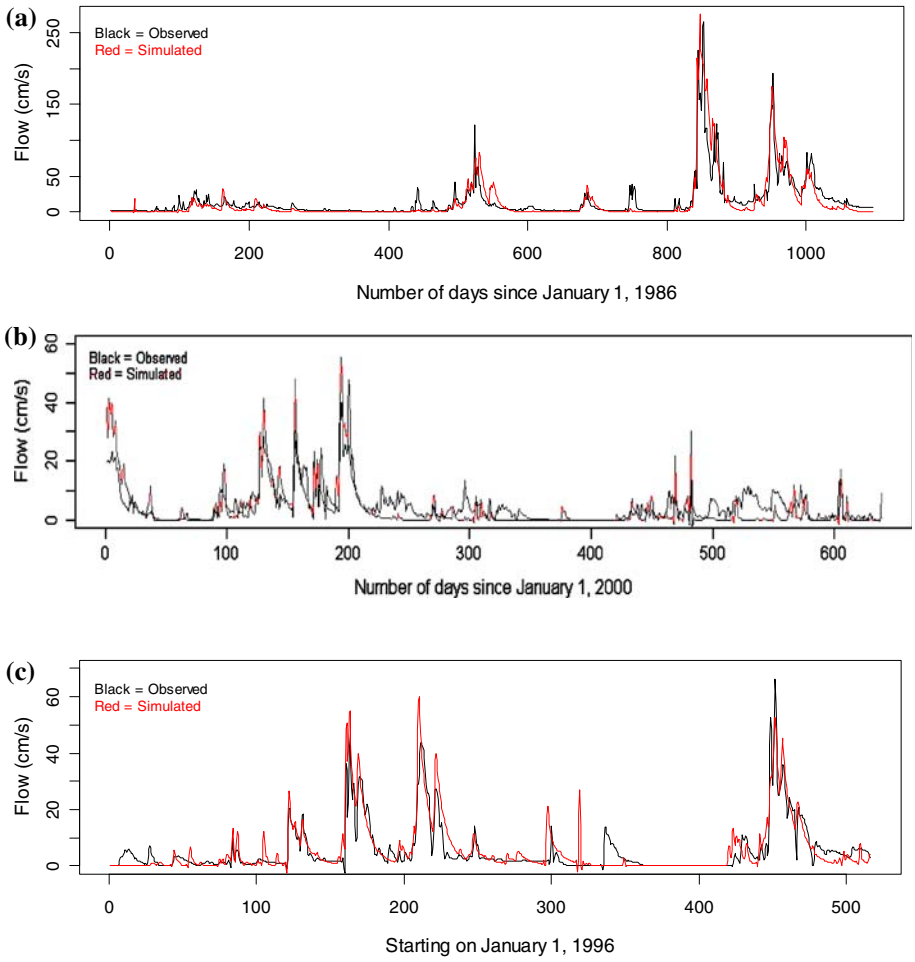

Fig. 9 Observed and simulated hydrographs of the Nyando River. (**a**) calibration run obtained with model-forced with rain gauge observed data; (**b**) validation run when model input rainfall was SBRE; and (**c**) simulated and observed flows when the model was calibrated with SBRE

performance was poor for the dry year. The lower performance of the model for the drier year was attributed to the way the hydrologic model was calibrated. During calibration, the RMSE of the difference between simulated and observed flows was minimized; models calibrated in such a manner places a higher value on matching the high flow than the average flows. The overall water balance agrees to within 18% of the observed flows. The hydrologic model calibrated with GORE data could be driven with SBRE as input rainfall for the Nyando with a notable loss of predictive skills, in contrast to when GORE data were used. We recalibrated the hydrologic model with SBRE data from January 1996 to June 1997. Simulated streamflow with the model driven with the SBRE had comparable skills with the GORE-forced simulations (NSCE = 0.74 and NSCE = 0.75, and RMSE = 0.18 and 0.42, respectively). GeoSFM SBRE-calibrated simulated flows had a minor positive bias (+7.4%), whereas the GORE-calibrated model flows were significantly negatively biased (−18.0%). This suggested that for the Nyando basin the hydrologic model should be calibrated with remotely sensed rainfall estimates if the model is to be used with such data.

The Gash River is seasonal, and it is located in an area that is dryer than the other three basins that were modeled for this study. In the case of the Gash River we had only SBRE data for both model calibration and validation. We had 6 years of observed streamflow data collected at the Kassala town gauging station. We used data from January 1998 to December 2001 to calibrate the model and we used the remaining 2 years of streamflow data for the validation. Figure 10a, b show modeled and observed hydrographs for the Gash River at Kassala for the calibration and validation periods. The agreement between simulated and observed flows obtained during the verification period was comparable to the agreement during the model calibration period. That suggests that the SBRE is an acceptable rainfall dataset for input to hydrologic and flood forecasting models for the Gash River.

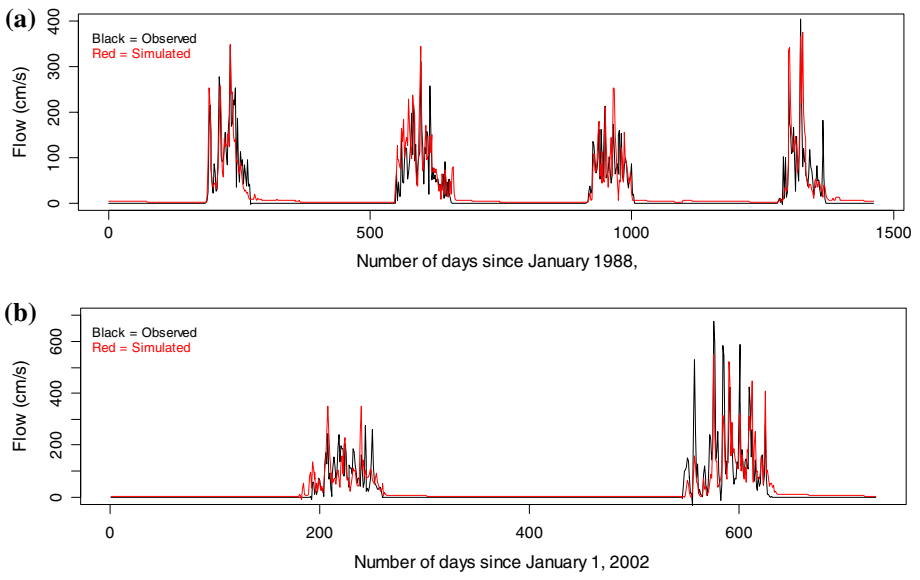

Fig. 10 Gash River observed and simulated hydrographs obtained when the model was calibrated with remotely sensed rainfall data (**a**) the calibration period, and (**b**) the validation period

5 Conclusion

Global coverage of remotely sensed rainfall estimates is becoming available. We have investigated the fitness of such data for streamflow modeling. Four basins that cover a wide range of hydro-climatic and physiographic conditions (from arid to tropical environments) were investigated. Streamflow was simulated with the GeoSFM, and calibrated using combinations of rain gauge measured and remotely sensed rainfall estimates. We also compared remotely sensed and gauge-estimated basin-wide mean areal precipitation. On daily time scales, the two rainfall estimates were weakly correlated, whereas the match between monthly accumulated rainfall values was excellent. Overall the remotely sensed rainfall estimates had only a small under-estimation bias. This suggests that the remotely sensed rainfall estimates are an excellent source of rainfall data for modeling processes with monthly and longer time scales.

A distributed hydrologic model was calibrated for three basins using daily GORE data and forced with daily SBRE data. Simulated streamflow for the basins showed that a slight rainfall bias was amplified into a much larger streamflow bias for one basin (Se Done). In the Nam Ou and Nyando basins there was no significant difference between streamflow simulated with GORE or SBRE. Our results concur with the point presented by other researchers (e.g., Hughes 2006) that SBRE cannot be used with confidence with GORE-calibrated hydrologic models without a model recalibration with SBRE. The performance of the hydrologic model, when calibrated with SBRE, was comparable to the simulated streamflow obtained when the model was calibrated with GORE. It is therefore justifiable to suggest that SBRE can be used to drive hydrologic models for streamflow prediction if the hydrologic model is calibrated with SBRE.

Acknowledgements The financial support of the USAID's Office of U.S. Foreign Disaster Assistance (OFDA) is gratefully acknowledged. The authors thank the Mekong River Commission for providing the Nam Ou and Se Done basins streamflow and rainfall data. Thanks are extended to two anonymous reviewers for helpful suggestions that contributed to improving the originally submitted version.

References

Artan G, Verdin J, Asante K (2001) A wide-area flood risk monitoring model. Fifth international workshop on application of remote sensing in hydrology. Montpellier, France, October 2–5

Chow VT, Maidment D, Mays L (1988) Applied Hydrology. McGraw-Hill Book Company, New York

Duan Q, Gupta VK, Sorooshian S (1992) Effective and efficient global optimization for conceptual rainfall-runoff models. Water Resour Res 28(4):1015–1031

FAO (Food and Agriculture Organization of the United Nations) (1995) Digital soil map of the world and derived soil properties. CD-ROM, version 3.5, November 1995

Gesch DB, Verdin LK, Greenlee SK (1999) New land surface digital elevation model covers the Earth. EOS Trans Am Geophys Union 80(6):69–70

Grimes DIF, Diop M (2003) Satellite-based rainfall estimation for river flow forecasting in Africa. I: rainfall estimates and hydrological forecasts. Hydrol Sci J 48(4):567–584

Guetter AK, Georgakakos KP, Tsonis AA (1996) Hydrologic applications of satellite data: 2. Flow simulation and soil water estimates. J Geophys Res 101(D21):26527–26538

Hanks J, Ashcroft GL (1980) Applied soil physics. Springer-Verlag, New York

Hansen VE, Israelson OA, Stingham G (1979) Irrigation principles and practice. John Wiley & Sons, New York

Herman A, Kumar V, Arkin P, Kousky J (1997) Objectively determined 10-day African rainfall estimates created for famine early warning systems. Int J Remote Sens 18(10):2147–2159

Hong Y, Hsu K, Gao X, Sorooshian S (2004) Precipitation estimation from remotely sensed imagery using Artificial Neural Network-Cloud Classification System. J Appl Meteorol 43:1834–1853

Hong Y, Hsu K, Moradkhani H, Sorooshian S (2006) Uncertainty quantification of satellite precipitation estimation and Monte Carlo assessment of the error propagation into hydrologic response. Water Resour Res 42(8): W08421, doi:10.1029/2005WR004398 10.1029/2005WR004398

Hossain F, Anagnostou EN (2004) Assessment of current passive-microvawe and infrared-based satellite rainfall remote sensing for flood prediction. J Geophys Res 109(D07102):1–14

Huffman GJ, Adler RF, Bolvin DT, Gu G, Nelkin EJ, Bowman KP, Hong Y, Stocker EF, Wolff DB (2007) The TRMM multi-satellite precipitation analysis: quasi-global, multi-year, combined-sensor precipitation estimates at fine scale. J Hydrometeorology 8(1):38–55

Hughes DA (2006) Comparison of satellite rainfall data with observations from gauging stations networks. J Hydrol 327:399–410

Jonkman SN (2005) Global perspectives on loss of human life caused by floods. Nat Hazards 34:151–175

Joyce RJ, Janowiak JE, Arkin PA, Xie P (2004) CMORPH: A method that produces global precipitation estimates from passive microwave and infrared data at high spatial and temporal resolution. J Hydrometeorology 5:487–503

Loveland TR, Belward AS (1997) The IGBP-DIS global 1 km land cover data set, discover first results. Int J Remote Sens 18(5):3289–3295

McCollum J, Gruber A, Mamoudou B (2000) Discrepancy between gauges and satellite estimates of rainfall in Equatorial Africa. J Appl Meteorol 39(5):666–679

Nash EJ, Sutcliffe JV (1970) River flow forecasting through conceptual models part I—a discussion of principles. J Hydrol 10(3):282–290

Nijssen B, Lettenmaier DP (2004) Effect of precipitation sampling error on simulated hydrological fluxes and states: anticipating the global precipitation measurement satellites. J Geophys Res Atmos 109(D2) Art. No. D02103, doi:10.1029/2003JD003497

OCHA (2002) Kenya - floods OCHA situation report No. 1, http://wwwnotes.reliefweb.int/w/rwb.nsf, ReliefWeb, United Nations Office for the Coordination of Humanitarian Affairs of the UN (OCHA)

OCHA (2003) Flooding in Kassala state information bulletin no. 1.http://wwwnotes.reliefweb.int/w/rwb.nsf, ReliefWeb, United Nations Office for the Coordination of Humanitarian Affairs of the UN (OCHA)

Olivera F, Maidment D (1999) Geographic information systems (GIS)-based spatially distributed model for runoff routing. Water Resour Res 35(4):1155–1164

Pielke RA Jr, Downton MW (2000) Precipitation and damaging floods: trends in the United States, 1932–97. J Clim 13:3625–3637

Plate EJ, Insisiengmay T (2002) Keynote lecture: early warning system for the Mekong River. Second international symposium on flood defence. Beijing, Sept. 10–13

Senay GB, Verdin J (2003) Characterization of yield reduction in ethiopia using a GIS-based crop water balance model. Can J Remote Sens 29(6):687–692

Sorooshian S, Hsu K, Gao X, Gupta HV, Imam B, Braithwaite D (2000) Evaluation of PERSIANN system satellite-based estimates of tropical rainfall. Bull Am Meteorol Soc 81:2035–2046

Tsintikidis D, Georgakakos KP, Artan GA, Tsonis AA (1999) Mean areal rainfall estimation and hydrologic response using METEOSAT data over the Blue Nile region. J Hydrol 221:97–116

Verdin J, Klaver R (2002) Grid cell based crop water accounting for the famine early warning system. Hydrol Proc 16:1617–1630

Vicente GA, Scofield RA, Menzel WP (1998) The operational GOES infrared rainfall estimation technique. Bull of the Am Meteorol Soc 79:1883–1898

Vrugt JA, Gupta HV, Bastidas LA, Bouten W, Sorooshian S (2003) Effective and efficient algorithm for multiobjective optimization of hydrologic models. Water Resour Res 39(8):1214, doi: 10.1029/2002WR001746

Wilk J, Kniveton D, Andersson L, Layberry R, Todd MC, Hughes D, Ringrose S, Vanderpost C (2006) Estimating rainfall and water balance over the Okavango River Basin for hydrological applications. J Hydrol, doi:10.1016/j.jhydrol.2006.04.049

Xie P, Arkin AP (1997) Global precipitation: a 17-year monthly analysis based on gauge observations, satellite estimates, and numerical model outputs. Bull Am Meteorol Soc 78(11):2539–2558